Tidal currents of global tidal models tested using estimates from ocean acoustic tomography

B.D. Dushaw *Applied Physics Laboratory, University of Washington, Seattle, WA USA*

ABSTRACT

As part of a project led by D. Stammer for assessing the qualities, relative merits, etc. of eleven global tidal models (Stammer et al., Richman et al., this conference), harmonic constants of tidal currents derived from recent tidal models are compared to harmonic constants estimated from ocean acoustic tomography. Data from four acoustic tomography arrays deployed for various exeriments over the past 30 years in the North Pacific and North Atlantic are used. As a measurement technique employing reciprocal acoustic signals that cycle throughout the water column and traverse O(500-km) distances, acoustic tomography offers a high-precision measurement of barotropic currents, tidal currents in particular. Baroclinic tidal currents negligibly influence these measurements. Previous comparisons of tidal current harmonic constants to tidal models have shown that tomography can accurately measure the harmonic constants of at least the eight largest tidal constituents. While some of the tidal models are constrained by observations and some are hydrodynamic, so that tidal currents are inherently a part of the tidal solution, none of the tidal models are constrained by measurements of tidal currents. The new comparisions between measured and model tidal harmonic constants are generally favorable, with most models being "about" right. Near Hawaii, small systematic differences between measured and modeled harmonic contants (amplitude and phase) suggest some aspect of the tidal models may be improved (missing or deficient physics), but the reasons for those differences are unknown at this time. In any case, insofar as these "spot" comparisons can determine, predictions of tidal currents derived from many of the modern global tidal models appear to be reasonably accurate, in the open ocean at least.

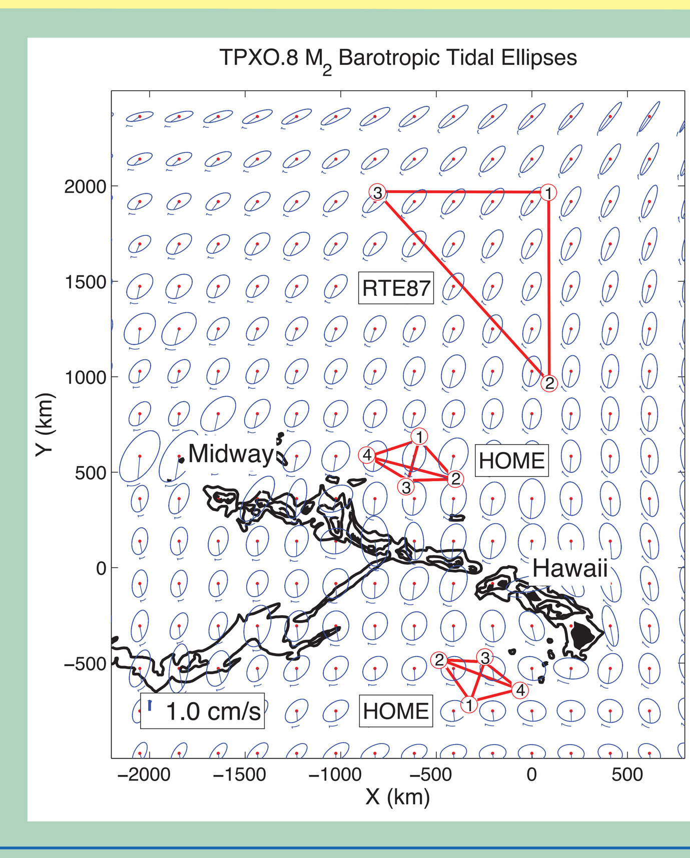

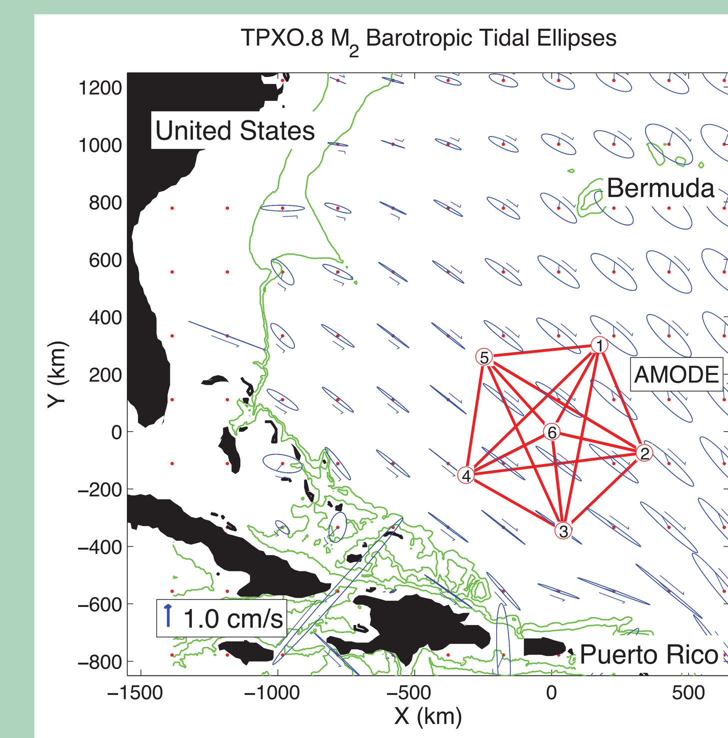

TOMOGRAPHY BASICS

Sound travels faster in warm water than in cold water. By measuring the travel time of sound over a known path, the sound speed and thus temperature can be determined. Each acoustic travel time represents the path integral of the sound speed (temperature) and water velocity. As the sound travels along a ray path, it inherently averages these properties of the ocean, heavily filtering along-path horizontal scales shorter than the path length. A 1°C change in temperature roughly corresponds to a 4 m/s change in sound speed, although this scale factor is somewhat temperature dependent. Over a 1000-km range, a depth-averaged temperature change of 10 m°C is easily measured as a 20-ms travel time change. (Munk, Worcester, and Wunsch, 1995)

Sound travels faster with a current than against. By measuring the reciprocal travel times in each direction along a path, the absolute water velocity can be determined, and the effects of temperature can be excluded. Currents (1 cm/s) have a much smaller signal than sound speed (1 m/s).

Sound speed is also weakly affected by salinity. A 1 PSU change in salinity corresponds to a 1 m/s change in sound speed. Normal variations in salinity in the ocean have an insignificant effect on sound speed insofar as long-range acoustics are concerned.

TIDAL MODELS

Currents corresponding to the tomography measurements were computed from eleven global tidal models. In many cases only the M_2 constituent was made available, or a particular model was only computed for M_2. Some of the model file sizes are rather large. Some models consider elevation only, with currents computed after the fact. Other models are hydrodynamic with currents computed as a part of the tidal solution.
(Red: Assimilating Black: Non-Assimilating)

1) TPXO (Egbert/OSU) An assimilative barotropic tide model, hydrodynamic, with many constituents. 1/30° resolution.

2) STORMTIDE (Müller et al. 2012) A non-assimilative ocean circulation and tide model, from which the barotropic tides extracted. Atmospheric as well as tidal forcing. 1/10° resolution.

3) HIM (Arbic et al.) A non-assimilative barotropic model updated from Arbic et al. 2004. 1/8° resolution.

4) HAMTIDE (Stammer et al./Hamburg, DE) An assimilative barotropic tide model. 1/8° resolution.

5) LEEDS (Griffiths/Leeds Univ., UK) A non-assimilative barotropic tide model, STM-1B. 1/12° resolution.

6) OTIS-GN (Green and Nycander 2013) A non-assimilative barotropic tide model. 1/8° resolution.

7) NSWC (Schwiderski ca. 1980) From Schwiderski's classic paper. An assimilative barotropic model; M_2 only. 1° resolution.

8) GOT4.7 (Ray 2001) An empirical tidal analysis with many constituents. Currents computed post hoc by least-squares inversion of momentum and continuity equations. 1/2° resolution.

9) OTIS-ERB (Egbert, Ray, and Bills 2004) A non-assimilative barotropic model. 1/12° resolution.

10) HYCOM (Arbic et al. 2010, 2012; Shriver et al. 2012) Non-assimilative. Barotropic tides extracted from a model which includes many layers and atmospheric as well as tidal forcing. 1/12° resolution, subsampled to 1/4° resolution.

11) FES 2012 (Lyard/LEGOS, Carrere et al. 2012, FR) A hydrodynamic barotropic model with assimilation of altimeter data. Unstructured global mesh with resolution a few km in coastal regions to 25 km in the deep ocean. 33 constituents, 1/16° resolution.

COMPARISONS TO EIGHT CONSTITUENTS: M_2 to Q_1

The precision of the tomographic measurements allows the first eight tidal constituents to be resolved: M_2, S_2, N_2, K_2, O_1, K_1, and even P_1 and Q_1. While the tidal comparisons mainly focus on M_2, the comparison to the other constituents illustrates two points:

First, the resolution of the rather small constituents P_1 and Q_1, with both amplitude and phase in agreement with models, demonstrates the precision of the observations.

Second, although the M_2 comparisons indicate that the measured amplitude is systematically smaller than modeled in some regions, particularly near Hawaii, this bias is not so apparent in the results for the other constituents. The discrepancy would appear to be more of a modeling problem than a measurement problem.

HOME Northern Array, Path 1,3
Southward current

Amplitude (cm/s)

	TOMOGRAPHY	TPXO 8-Atlas	FES2012
M2	1.55±0.02	1.67	1.74
S2	0.73	0.76	0.71
N2	0.30	0.30	0.28
K2	0.25	0.21	0.24
O1	0.21	0.25	0.27
K1	0.32	0.44	0.42
P1	0.16	0.13	0.13
Q1	0.03	0.04	0.05

Phase (°)

	TOMOGRAPHY	TPXO 8-Atlas	FES2012
M2	10±1	12	10
S2	38±2	40	40
N2	12±4	10	10
K2	28±5	35	38
O1	354±5	11	10
K1	350±4	10	16
P1	350±7	10	12
Q1	13±40	7	10

HOME Southern Array, Path 2,4
Southeastward current

Amplitude (cm/s)

	TOMOGRAPHY	TPXO 8-Atlas	FES2012
M2	1.22±0.02	1.32	1.45
S2	0.55	0.58	0.58
N2	0.23	0.25	0.27
K2	0.14	0.16	0.16
O1	0.21	0.23	0.25
K1	0.30	0.35	0.32
P1	0.11	0.10	0.10
Q1	0.04	0.05	0.05

Phase (°)

	TOMOGRAPHY	TPXO 8-Atlas	FES2012
M2	298±1	294	295
S2	311±2	310	313
N2	286±5	289	286
K2	308±9	305	308
O1	113±6	110	101
K1	140±4	144	140
P1	157±11	142	138
Q1	110±32	93	86

RTE87 - M_2 Tidal currents in the central North Pacific

Tidal currents were measured along the three legs of the RTE87 tomography triangle in summer 1987 (Dushaw et al. 1995). The path lengths were 750, 1000, and 1250 km. The record lengths were about 120 days with measurements obtained every 2 hours on every fourth day. The analysis procedure was to first solve for barotropic current from the acoustic data, and then do a tidal analysis of the time series of barotropic current using weighted least squares. The uncertainties indicated below are the formal estimates for the uncertainty from this least squares analysis. The non-tidal barotropic currents were an order of magnitude smaller than the tidal currents.

Zonal Current (cm/s,°)

	Amplitude	Phase
TOMOGRAPHY	1.31±0.03	223±1
Schwiderski	1.28	222
TPXO 8	1.24	221
STORMTIDE	0.97	218
HIM	1.15	226
HAMTIDE	1.26	220
LEEDS	0.83	254
OTIS-GN	1.31	219
NSWC	1.22	221
GOT4.7	1.25	222
ERB	1.15	235
HYCOM	1.29	222
FES2012	1.33	222

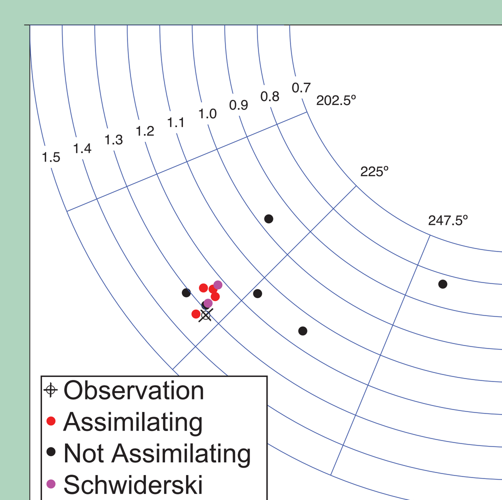

Meridional Current (cm/s,°)

	Amplitude	Phase
TOMOGRAPHY	1.54±0.04	176±2
Schwiderski	1.39	177
TPXO 8	1.57	173
STORMTIDE	1.53	171
HIM	1.62	175
HAMTIDE	1.60	174
LEEDS	1.60	185
OTIS-GN	1.74	167
NSWC	1.42	176
GOT4.7	1.58	174
ERB	1.69	174
HYCOM	1.69	165
FES2012	1.59	173

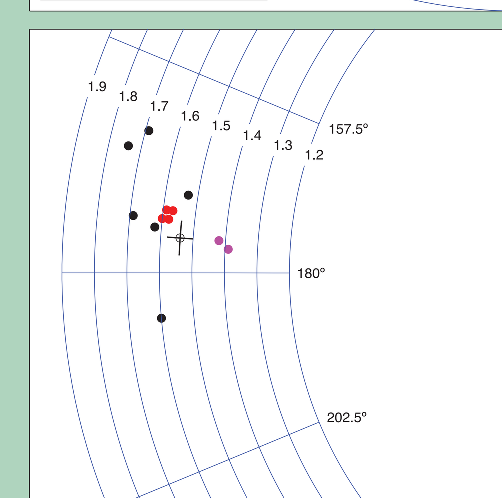

AMODE - M_2 Tidal currents in the western North Atlantic

Tidal currents were measured along each of the fifteen legs of the Acoustic Mid-Ocean Dynamics Experiment (AMODE) tomography triangle in 1991-2. The path lengths were 350-660 km. The record lengths were about 150-250 days with measurements obtained every 3 hours on every fourth day. The non-tidal barotropic currents were comparable in magnitude to the tidal currents, mainly due to mesoscale activity. Harmonic constants from the two paths along the major (Path 2,5) and minor axes (Path 1,4) of the tidal elipses are shown here.

Major Axis Current (cm/s,°)

	Amplitude	Phase
TOMOGRAPHY	1.15±0.02	283±1
TPXO 8	1.34	282
STORMTIDE	1.33	280
HIM	1.18	279
HAMTIDE	1.34	283
LEEDS	0.92	271
OTIS-GN	1.19	292
NSWC	1.08	284
GOT4.7	1.35	283
ERB	1.13	289
HYCOM	0.98	290
FES2012	1.40	294

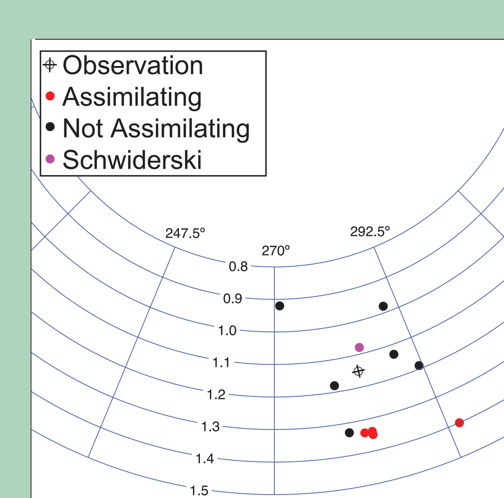

Minor Axis Current (cm/s,°)

	Amplitude	Phase
TOMOGRAPHY	0.25±0.01	252±3
TPXO 8	0.28	248
STORMTIDE	0.29	230
HIM	0.19	226
HAMTIDE	0.28	250
LEEDS	0.30	214
OTIS-GN	0.23	245
NSWC	0.13	39
GOT4.7	0.29	256
ERB	0.24	237
HYCOM	0.20	224
FES2012	0.38	275

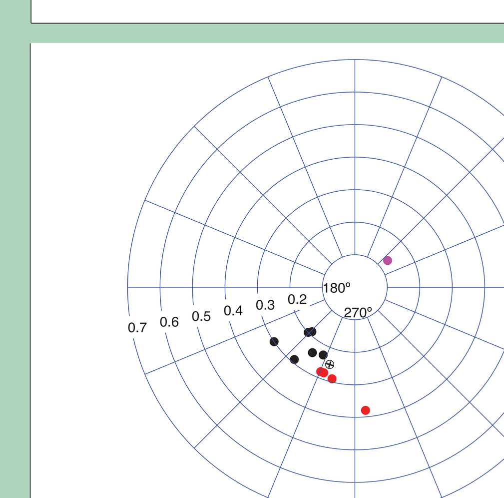

HOME - M_2 Tidal currents around the Hawaiian Ridge

The Hawaiian Ocean Mixing Experiment (HOME) tomography arrays were designed to measure barotropic tidal currents in conjunction with pressure measurements. Record lengths were about 150 days. The HOME array was first deployed north of Hawaii for about 1 year, and then moved south of Hawaii for a year. The northern array suffered instrument failure, leaving only a single path with reciprocal transmissions. The southern array functioned normally.

The arrays were designed to measure radiation of internal tides from the Hawaiian Ridge, hence the longest path of the array diamond was aligned with the Ridge. Currents reported here are along this path and the short path perpendicular to it.

HOME North

North Path 1,3 Current (cm/s,°)

	Amplitude	Phase
TOMOGRAPHY	1.55±0.02	10±1
TPXO 8	1.67	12
STORMTIDE	1.57	14
HIM	1.85	16
HAMTIDE	1.72	14
LEEDS	1.67	27
OTIS-GN	1.98	6
NSWC	1.58	17
GOT4.7	1.68	13
ERB	1.86	14
HYCOM	1.78	4
FES2012	1.74	10

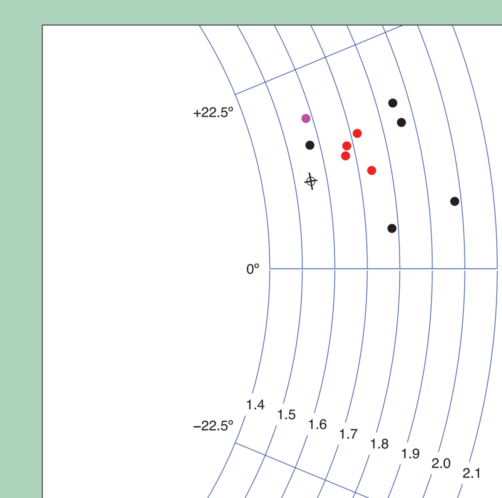

HOME South

South Path 2,4 Current (cm/s,°)

	Amplitude	Phase
TOMOGRAPHY	1.22±0.02	298±1
TPXO 8	1.32	294
STORMTIDE	1.47	298
HIM	1.38	295
HAMTIDE	1.30	294
LEEDS	1.43	313
OTIS-GN	1.41	279
NSWC	1.38	308
GOT4.7	1.30	294
ERB	1.39	299
HYCOM	1.55	295
FES2012	1.45	295

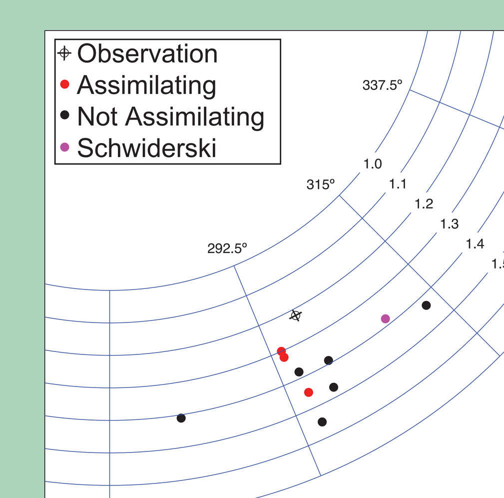

South Path 1,3 Current (cm/s,°)

	Amplitude	Phase
TOMOGRAPHY	1.00±0.02	207±1
TPXO 8	1.21	208
STORMTIDE	1.17	212
HIM	1.37	208
HAMTIDE	1.21	206
LEEDS	1.30	224
OTIS-GN	1.43	195
NSWC	1.31	215
GOT4.7	1.23	206
ERB	1.32	205
HYCOM	1.30	199
FES2012	1.29	207

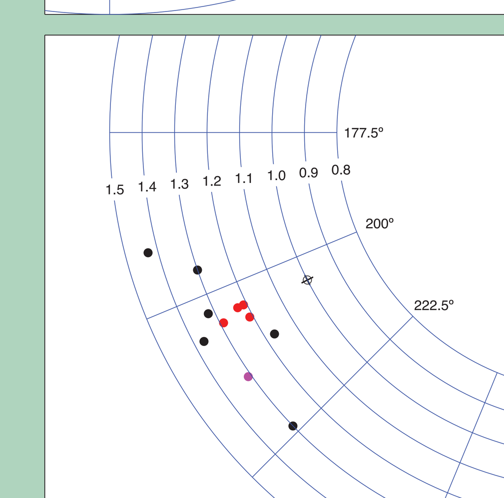

Tidal Energy Flux: (<p'u'>,<p'v'>)

The energy flux of the tide can be analytically computed from the harmonic constants for elevation and currents. The field of M_2 energy flux computed from the TPXO.3 tidal model for the M_2 constituent near Hawaii shows that most of the tidal energy flows around Hawaii. This energy flux is determined by the phase of elevation relative to current, hence the motivation to obtain accurate measurements of both of these quantities near the Hawaiian Ridge during HOME.

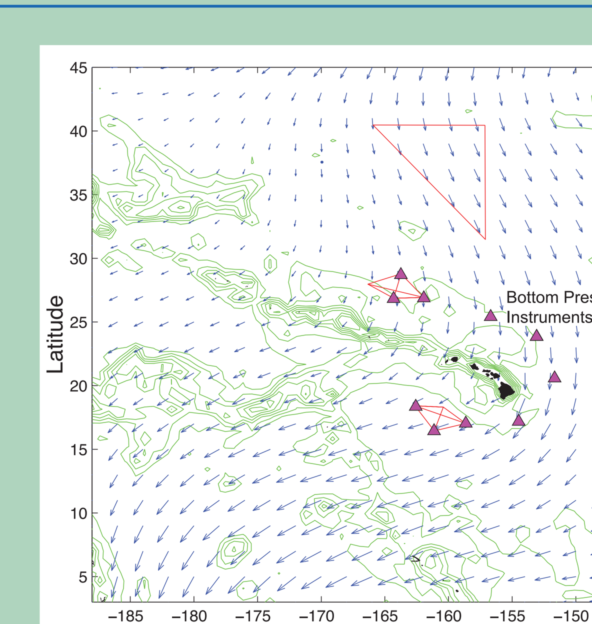

TIDAL VORTICITY

By Stokes' Theorem, integration of current around a closed loop is equal to the areal-average relative vorticity. A small vorticity is induced by the tides, primarily by tidal elevation stretching the vortex lines. To a lesser extent, currents contribute to vorticity, through the "beta-v" (β=df/dy) term and through flow over varying topography. The dominant term is tidal elevation, so tidal vorticity is roughly in phase with elevation (Dushaw et al 1997).

$$\zeta = \frac{f\eta}{H} - \frac{(f/H)\nabla H \cdot \mathbf{u}}{i\omega} + \frac{\beta v}{i\omega}$$

$\eta = (30\ \text{cm}, 5°)$ Sea surface height relative to the bottom.

$\zeta = (1\text{–}2 \times 10^{-9}\ \text{s}^{-1}, 350°)$ "Theoretical" vorticity.

TPXO.2 M_2 Tidal Elevation Amplitude and Phase

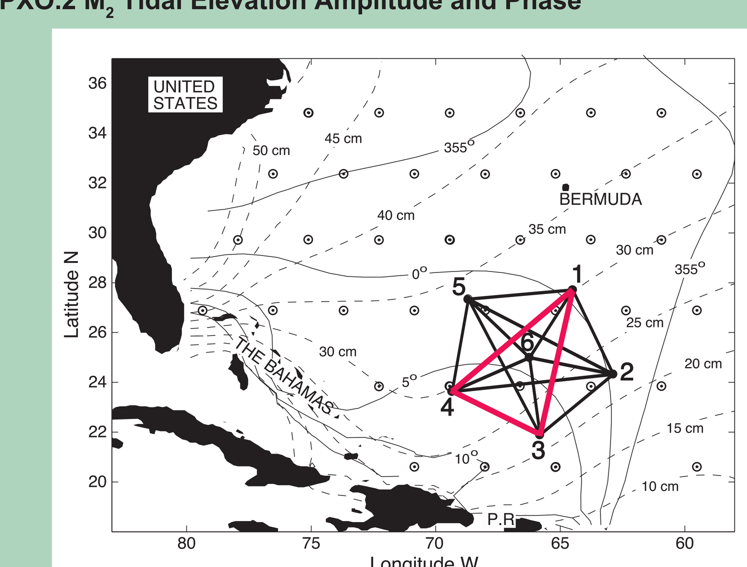

AMODE tidal vorticity: integration around 5 isoceles triangles

Tidal vorticity is estimated for the five isosceles triangles of the AMODE array. This vorticity is tiny: four orders of magnitude less than planetary vorticity. The measurement is at the limits of tomography and relies on the leverage of tidal analysis.

Amplitude (10^{-9} 1/s)

Triangle	Tomography	Theory	TPXO8	FES2012	HAM	GOT4.7
1,3,4	0.9 ± 0.8	1.0	0.6	4.5	0.4	0.7
2,4,5	5.6 ± 1.6	1.9	1.9	2.9	2.4	1.8
3,5,1	5.6 ± 1.4	1.5	1.3	5.2	1.5	0.7
4,1,2	7.1 ± 1.1	1.0	0.8	3.8	1.2	1.1
5,2,3	8.1 ± 1.7	1.3	1.4	2.5	1.7	0.3

Phase (°)

Triangle	Tomography	Theory	TPXO8	FES2012	HAM	GOT4.7
1,3,4	210 ± 55	351	262	290	335	311
2,4,5	277 ± 17	356	344	329	356	374(14)
3,5,1	309 ± 15	346	309	292	338	356
4,1,2	276 ± 9	334	300	294	339	333
5,2,3	294 ± 12	350	334	311	328	301

Positive relative vorticity is anticlockwise.

Measured vorticity has larger amplitude and leads theory and most models by 10-50°. The models mostly reflect the basic theory. The high-resolution FES2012 model vorticities are more similar to the observations, but currents from this model are not quite as accurate as other models in the AMODE region. The uncertainties in the measurements are large.

REFERENCES

Dushaw, B. D., B. D. Cornuelle, P. Worcester, B. M. Howe, and D. S. Luther, 1995: Barotropic and baroclinic tides in the central North Pacific Ocean determined from long-range reciprocal acoustic transmissions. *J. Phys. Oceanogr.*, **25**, 631-647.

Dushaw, B. D., G. D. Egbert, P. Worcester, B. Cornuelle, B. Howe, and K. Metzger, 1997: A TOPEX/POSIEDON global tidal model (TPXO.2) and barotropic tidal currents determined from long-range acoustic transmissions. *Progress in Oceanography*, **40**, 337-367.

Munk, W., P. Worcester, and C. Wunsch, 1995: *Ocean Acoustic Tomography*, Cambridge University Press, Cambridge.